Ab initio study of molecule transport characteristics based on nonequilibrium Green's function theory

F. Jiang,[1] Y. X. Zhou,[1] H. Chen,[1,*] R. Note,[2] H. Mizuseki,[2] and Y. Kawazoe[2]
[1]*Physics Department, Fudan University, Shanghai 200433, People's Republic of China*
[2]*Institute for Materials Research, Tohoku University, Sendai 980-8577, Japan*
(Received 30 March 2005; revised manuscript received 5 July 2005; published 12 October 2005)

We use a self-consistent method to study phenyl dithiol transport from the first-principles calculations. The calculated current and differential conductance are supported by the famous experimental results [Reed *et al.*, Science **278**, 252 (1997)]. We investigate the coupling effects between the sulfur atom and the metal surface by adjusting their distance in a very small range, and find that the charge carriers responsible for the initial rise of the current can be changed from holes to electrons. We calculate the *I-V* behaviors of the naphthalene-dithiol and anthracene-dithiol dressed by the gold electrodes. The numerical results present the quantum behaviors that are in agreement with the recent experiments for the anthrylacetylene by Zareie *et al.* [Nano Lett. **3**, 139 (2003)].

DOI: 10.1103/PhysRevB.72.155408 PACS number(s): 73.23.−b, 85.65.+h, 31.15.Ar

I. INTRODUCTION

Recently, the search for new active molecular devices becomes a worldwide effort as these devices represent the ultimate size limit of functional devices. The current-voltage (*I-V*) characteristics of the molecular devices show profound potential for applications, including the negative differential resistance and switches, etc. Several experimental groups reported measurements of the *I-V* characteristics of small numbers of molecules.[1–13] These developments attracted much attention from the semiconductor industry, and caused a great interest in modelling and understanding the capabilities of the molecular conductor from the basic scientific and applied point of view.[14–31]

Traditionally, electronic transport phenomena are studied in the context of bulk semiconductor devices, the theoretical description of which is largely built on two premises, the effective-mass approximation and the Boltzmann transport equation. The situation changes dramatically for the molecular devices. At the molecular scale, the effective-mass approximation breaks down and the electronic structure of the system must be taken explicitly into account. Microminiaturization of the electronic devices to the molecular scale brings another complication in the transport study compared with macroscopic systems, the treatment of contacts. In macroscopic transport, the details of contacts are usually not important. However, for the devices of molecular dimension, the contact becomes an important part of the device and the measured electronic characteristics depend on the details of the coupling between the molecule and the macroscopic electrode with the band structure. In a word, transport in molecular devices is different from that in semiconductor devices in two aspects, (1) the effect of the electronic structure and (2) the effect of contact. The rigorous treatment of molecular devices requires the inclusion of the semi-infinite gold contacts under bias. This calls for combining the theory of quantum transport with the theory of electronic structure starting from the first-principles calculations.

From the theoretical point of view, it is a serious challenge to accurately predict quantum transport properties of molecular devices in the first-principles level. The macroscopical electrodes and the organical molecule should be treated on an equal footing, with the whole open system, lead-molecule-lead, calculated self-consistently. Di Ventra[15] adopted the jellium model to deal with semi-infinity leads and Lippman-Schwinger equation to deal with the electronic structure, while Xue,[16] Damle,[17,18] and Taylor[19–21] adopted density functional theory (DFT) calculations for the central molecule and the basic group of the semi-infinity leads associated with nonequilibrium Green's function (NEGF) to deal with the transport problem. In Taylor's work, the quantum chemistry software Siesta provided the DFT calculation, while in the calculations of Damle and Xue the sophisticated quantum chemistry software GAUSSIAN98 did the same work. Both Taylor and Xue used tight-binding parameters obtained by fitting accurate augmented-plane-wave calculation of band structure to describe contacts of quasi-one-dimensional (quasi-1D) leads. Damle obtained the data from the finite cluster first, then resumed these data according to the lattice symmetry, and finally calculated the surface Green's function (SGF) of the three-dimensional (3D) lattice. Following Damle *et al.*[17,18] we adopt 3D lattice, based on DFT tight-binding model, to deal with electrode. We use the standard quantum chemistry software GAUSSIAN03,[32] of which the convergency is improved to a large extent, to calculate the electronic structure for both the organic molecule and the macroscopical electrodes and cooperate with the nonequilibrium Green's function theory to build electronic transport theory of the open system. At present the Gaussian software is designed only for the self-consistent calculations of the isolated system, used in the quantum chemistry. So it should be developed to deal with the quantum transport problem of the open system.[15–21]

The paper is organized as follows. In Sec. II, we give a detailed description of the theoretical formulism and the computational details. We use our code to study the transport characteristic of molecular devices such as phenyl dithiol (PDT), the naphthalene-dithiol, and the anthracene-dithiol in Sec. III. Finally, we summarize our work and give our expectations for the future work.

II. THEORETICAL FORMULA AND COMPUTATIONAL DETAILS

For the lead-molecule-lead system, coupling between the molecule and the leads plays a crucial role in quantum transport. Being computationally tractable, the whole system is partitioned into the molecule part and the lead part so that these two parts are dealt with separately. The nonequilibrium Green's function theory provides a powerful method to give a full description of transport phenomena.

The retarded Green's function satisfies the matrix equation

$$\sum_k (E^+ S_{i,k} - F_{i,k}) G^R_{k,j}(E) = \delta_{i,j}, \tag{1}$$

where E^+ denotes energy plus an infinitesimal imaginary part (usually 10^{-5} or 10^{-6}), S represents the orbital overlap matrix, and F the Fock matrix.

After partitioning Eq. (1) into the molecule part and the lead part, we obtain the Dyson equation

$$G^R_M = (E^+ S_M - F_M - \Sigma^R_1 - \Sigma^R_2)^{-1}, \tag{2}$$

where G^R_M, S_M, F_M are the retarded Green's function, overlap matrix and Fock matrix of the molecule part, respectively. $\Sigma^R_1(\Sigma^R_2)$, the retarded self-energy of the left-hand (right-hand) side, is calculated from SGF $g^R_1(g^R_2)$,

$$\Sigma^R_i = (E^+ S_{Mi} - F_{Mi}) g^R_i (E^+ S_{iM} - F_{iM}) \tag{3}$$

with $i=1,2$. The coupling matrices S_{Mi} and $F_{M,i}$ are extracted from the DFT calculation for the extended molecule (molecule with three Au atoms on each side).

In our calculation, the lead is considered as a truly three-dimensional one with the semi-infinite periodic bulk lattice. The SGF in $\vec{k}$ space representation is calculated iteratively in the gold FCC (111) direction

$$(g^R_{\vec{k}})^{-1} = E^+ S_{00} - F_{00} - (E^+ S_{01} - F_{01}) g^R_{\vec{k}} (E^+ S^\dagger_{01} - F^\dagger_{01}), \tag{4}$$

where S_{00}, F_{00} represent the overlap and Fock matrix of the surface layer in $\vec{k}$ space representation, and S_{01}, F_{01} represent the counterparts between the surface layer and the nearest layer. They are all calculated by DFT method through GAUSSIAN03. The SGF in the real space is obtained from the Fourier expansion

$$g^R_{s,ij} = g^R_s(\vec{r_i} - \vec{r_j}) = \frac{1}{N} \sum_{\vec{k}} g^R_{\vec{k}} e^{i\vec{k}\cdot(\vec{r_i} - \vec{r_j})}, \tag{5}$$

where N is the number of points in the two-dimensional (2D) Brillouin zone, or the number of unit cells in the lead surface (usually, 11×11 unit cell is enough).

The density matrix of the open system is the essential function of the whole self-consistent scheme. It can be achieved by the Keldysh Green's function

$$\rho = \int_{-\infty}^{\infty} dE[-iG^<(E)/2\pi], \tag{6}$$

$$-iG^< = G^R_M (f_1 \Gamma_1 + f_2 \Gamma_2) G^A_M. \tag{7}$$

The advanced Green's function $G^A = (G^R)^\dagger$, $f_1(f_2)$ is the Fermi distribution of the left (right) lead in equilibrium. $f_i(E) = 1/(e^{(E-\mu_i)/kT} + 1)$ with $\mu_1 = E_f - \frac{1}{2}eV$, $\mu_2 = E_f + \frac{1}{2}eV$, and the Fermi level of the bulk Au E_f. The zero point of the electrical potential is set at the symmetrical center of the lead-molecule-lead system. The broadening function of the left (right) lead $\Gamma_1(\Gamma_2)$, which denotes the finite lifetime of the electron, is a real symmetry matrix

$$\Gamma_{1(2)} = i(\Sigma^R_{1(2)} - \Sigma^A_{1(2)}). \tag{8}$$

With the help of the total density of states (DOS), the Fermi energy is accurately determined from the correct number of electron inside the molecule. Unfortunately, the DOS inside the highest occupied molecular orbital and/or lowest unoccupied molecular orbital (HOMO-LUMO) gap is quite small, making the precise location of the Fermi energy very sensitive to level broadening. So treating E_f as a "fitting parameter" around the value of the work function (5.31 eV) of the gold FCC structure in (111) direction may be a reasonable approximation at this stage of research work, when trying to explain the experimental *I-V* curve. In our work, E_f is -5.1 eV.

In the calculation the density matrix is partitioned into two parts

$$\rho = \rho^{\mathrm{eq}} + \rho^{\mathrm{neq}}, \tag{9}$$

where the equilibrium state contribution is obtained from the integration along the real axis from $-\infty$ to E_b (below the bottom energy of the molecule valence band) and the one along the semicircle from E_b to μ_1 in the complex contour, respectively (at zero temperature for simplicity),

$$\rho^{\mathrm{eq}} = -\frac{1}{\pi} I_m \left[\left(\int_{-\infty}^{E_b} + \oint_{E_b}^{\mu_1} \right) dE G^R_M(E) \right], \tag{10}$$

$$\rho^{\mathrm{neq}} = \frac{1}{2\pi} \int_{\mu_1}^{\mu_2} dE G^R_M \Gamma_2 G^A_M. \tag{11}$$

It is noted that the second part of Eq. (10) is the contribution from the valence electrons and its first part is from the deep core level electrons, which can be integrated by using $-i\eta$ to replace the self-energy. Without the density matrix evaluated accurately, the *I-V* curve will be trustless. To check the accuracy of the density matrix, the electron number of the molecule is the touchstone

$$N = \mathrm{Tr}(\rho S_M). \tag{12}$$

The molecule connected to the contacts under bias must keep neither the integer number of electrons, nor the neutral states. There are some charges transferred between the molecule and the metal electrodes. The absolute value of the transferred charges $|\delta n|$ for most metal-molecule combinations is usually much less than one and the charges transferred are accumulated on the contact surface. Getting the density matrix accurately, we can calculate the total current for coherent transport,

$$I = \frac{2e}{h}\int_{-\infty}^{\infty} dET(E,V)[f_2(E) - f_1(E)]$$

$$= \frac{2e}{h}\int_{-\infty}^{\infty} dE\ \mathrm{Tr}(\Gamma_1 G^R \Gamma_2 G^A)[f_2(E) - f_1(E)], \qquad (13)$$

where $T(E,V)$ is the transmission function.

The molecular DOS is connected to the imaginary part of the retarded Green's function,

$$\mathrm{DOS} = -\frac{1}{\pi}\,\mathrm{Im}\,\mathrm{Tr}(G_M^R S_M). \qquad (14)$$

In the calculation mentioned above, the inner cycle of GAUSSIAN03 is replaced by the cycle containing lead-molecule-lead open system under bias based on NEGF. The procedure for solution is summarized step-by-step as follows:

(1) For a particular device with contacts, all the matrices are expressed in the appropriate basis. The *ab initio* Hamiltonian matrix is obtained using GAUSSIAN03.

(2) Then compute the contact self-energy functions.

(3) For the self-consistent procedure, start with a guess for the density matrix of the molecule. The guess may be obtained from the converged density matrix of GAUSSIAN03 calculation for the isolated molecule.

(4) Calculate the density matrix using Eq. (9).

(5) Feedback the density matrix to Gaussian's main routine with the "field" option to present the electrical field along the transport direction due to the bias applied to the molecule, one obtains a new density matrix.

(6) Iterate step (4) and (5) until one obtains the converged density matrix within the acceptable accuracy, then use this matrix to calculate the terminal current and the DOS of the molecule.

In this paper, we adopt density functional theory with B3PW91 exchange-correlation potential and LANL2DZ basis to calculate the electronic structure and the Hamiltonian. The basis set associates with the effective core potential (ECP) which are specially suited for the fifth-row (Cs-Au) elements with considering the Darwin relativistic effect.

III. RESULTS AND DISCUSSIONS

The phenyl dithiol is one of the most intensively studied systems experimentally and theoretically for electron transport through molecules. Although great effort has been made theoretically to simulate the experimental *I-V* curve and conductance gap,[1,15,17] there is a big gap between the calculations and the experimental results, which needs further improvement.

With PDT connected to two gold leads, there are two kinds of geometric configurations usually. The sulfur atom sits directly on the top position of a surface gold atom or the hollow position of three nearest-neighbor surface gold atoms. As a conventionally accepted picture the latter is adopted in this paper, and the coupling between the organic molecule and the gold leads is obtained exactly from the DFT numerical calculation for the supermolecule, which includes three nearest-neighbor gold atoms of the sulfur atom on each side. The perpendicular distance between the sulfur atom and the Au FCC (111) surface plane is 2.0 Å, a usually acceptable distance. Figure 1 shows the PDT dressed by the gold electrodes. In the gold lead the parallel planes *ABC* are aligned in Au (111) direction, starting from the surface and extending to the infinite sequence *ABCABC*, etc., with lattice parameter 2.883 79 Å. We use 28 gold atoms as the calculated model (Fig. 1).[18] Seven atoms in the central hexagon of plane *B*, which are the nearest neighbors of three gold atoms in surface *A*, other 15 atoms around in plane *B*, which only play an auxiliary role to decrease the edge effect, and three gold atoms in plane *C*, which are the nearest neighbors of the central gold atom in plane *B*, for reducing the edge effect. The model is calculated by DFT method to extract the matrixes S_{00}, F_{00}, S_{01}, and F_{01} in Eq. (4). By using the tight-binding method, the SGF is achieved by Eqs. (4) and (5) for three gold atoms in surface *A* of the semi-infinite gold lead. The self-energy functions, which describe the influence of the electrodes on the central molecule, provide the important contribution to the self-consistent calculations of the open system. They are calculated by DFT and the tight-binding (for SGF) calculations [Eq. (3)], but not self-consistently obtained themselves in the open system, to avoid very heavy calculations. The more accurate calculation shows the self-energy functions are mainly determined by the distance between the S atom and Au surface, the charge effect is secondary. In the calculations, only zero temperature is concerned with for simplicity and the finite temperatures will not change the results in essence.

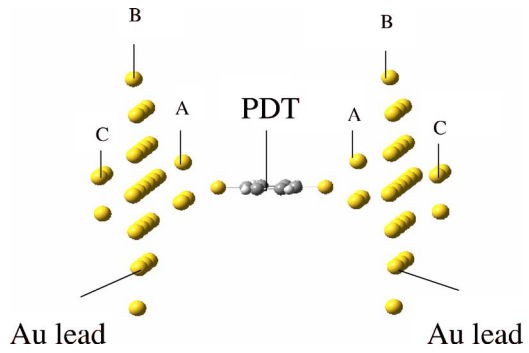

FIG. 1. (Color online) An open system, lead-PDT-lead. In the lead's calculation, three Au layers are used whose atom numbers are 3, 22, 3, respectively. The sulfur atom of PDT sits on the hollow position of three nearest neighbor gold atoms.

The lowest unoccupied molecular orbital, the highest occupied molecular orbital, and the related levels nearby of the isolated PDT are labelled in Fig. 2(a). Compared to the HOMO and LUMO positions of the isolated molecule (in the figure, HOMO is at −6.72 eV, LUMO is at −5.02 eV), both broadened HOMO and sharp LUMO are shifted in the lead-PDT-lead system. The situation is well expected since the LUMO of isolated PDT is localized on the phenyl ring, while its HOMO is delocalized over the molecule. It is reasonable since the states localized on the ring have little interaction with contacts that results in the longer lifetime of electrons, with small broadening and the sharp peaks in the DOS. In the HOMO-LUMO gap of the molecule-electrode system

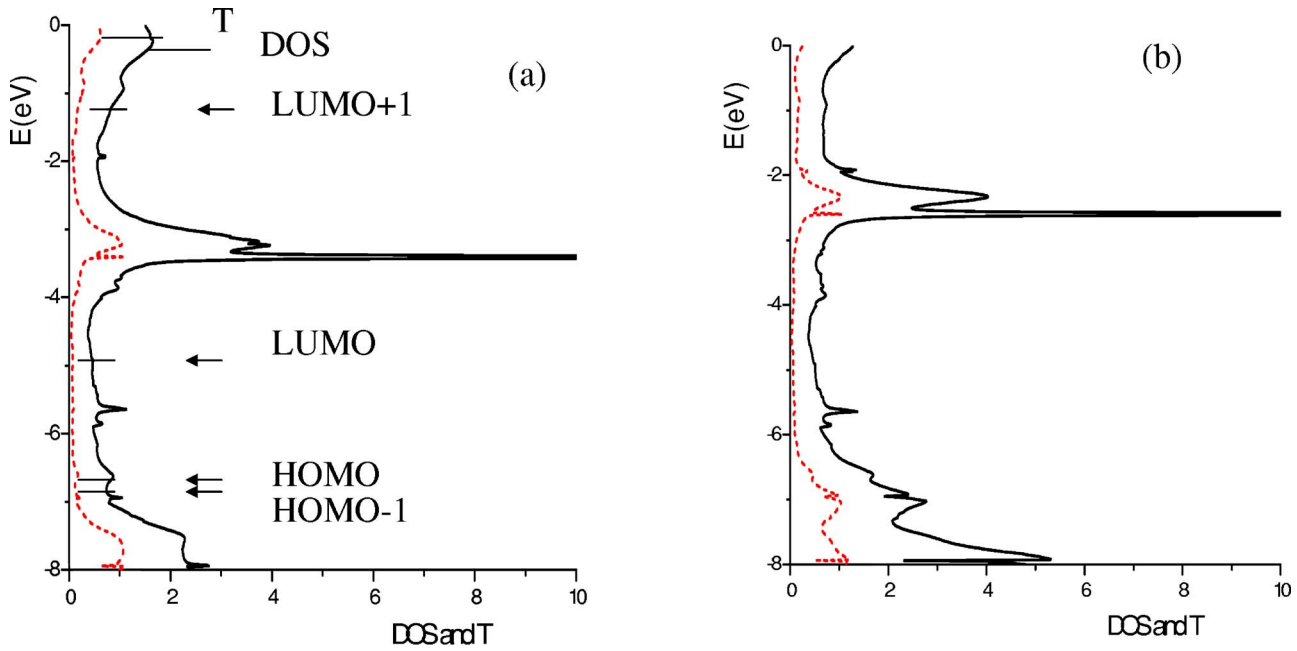

FIG. 2. (Color online) DOS (solid) and T (dashed) as functions of energy of PDT system with $V=0$ V. The horizontal lines show the energy levels of the isolated PDT. The distance between the sulfur atom and the Au FCC (111) surface plane is (a) 2.0 Å, (b) 2.1 Å.

there are many small states, called as the metal-induced gap states (MIGS), which are due to the hybridization of the metal surface states with the molecule states. The Fermi level E_f(−5.10 eV) is almost in the center of the HOMO-LUMO gap. The alpha electron number of the isolated PDT given by Gaussian is 26. Twenty of them are valence electrons, which give the main contribution to the current and the other six are deep core level electrons. In the open system of the closed-shell PDT the theoretical calculation shows the alpha electron number is over 25.8 and the beta electron number is the same. The charges transferred from the molecule to the metal electrodes $|\delta n|$ is less than 0.2. The fact that the number of states below the Fermi energy is equal to the number of electrons in the molecule does not require the electron number to be equal to an integer number. As mentioned above, a molecule connected to the circuit does not remain exactly neutral. It picks up a fractional charge depending on the work function of the metal and the distance between S atom and Au contact surface. The introduction of self-energy functions results in shift and broadening of energy levels, and the appearance of MIGS in the HOMO-LUMO gap. Despite the shift of HOMO is not small (0.7 eV), the broadening of energy levels tend to keep the system neutral.[33] At the beginning of the iteration process the initial guessed Fock matrix, which is the converged Fock matrix of the isolated molecule, does not keep the system electrical-neutral (the system often loses or gains more than one electron) without meeting the converged condition. With the iteration converged, the system reaches the state near the electrical-neutral condition.

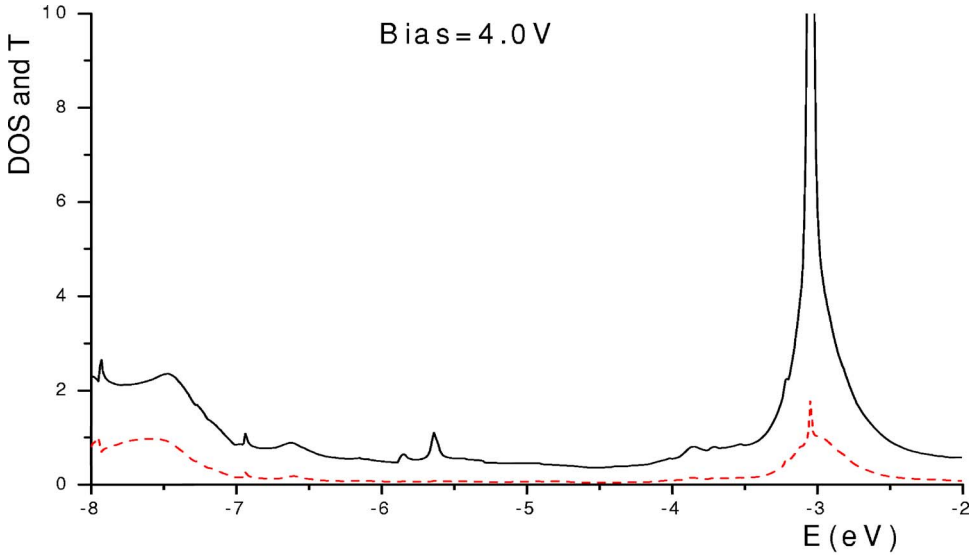

FIG. 3. (Color online) DOS and T of the lead-PDT-lead system with bias $V=4.0$ V. The distance between the sulfur atom and the Au (111) surface plane is 2.0 Å.

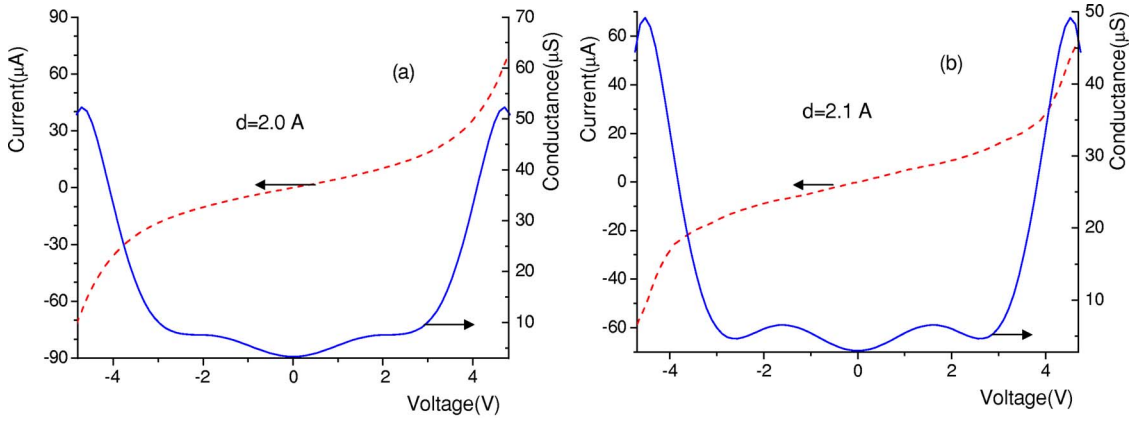

FIG. 4. (Color online) *I-V* (dashed) and differential conductance (solid) curves of the PDT system. The distance between the sulfur atom and the Au (111) plane is (a) 2.0 Å, (b) 2.1 Å.

In comparison with Fig. 2, which shows the DOS and T of PDT connected to two leads in equilibrium at bias $V=0$ V, Fig. 3 illustrates the positions of the peaks of DOS and T in nonequilibrium at bias $V=4.0$ V, that shows the peaks float up with the bias. In fact, with the bias below 3.0 V, the energy levels do not shift much since μ_2 does not get across the LUMO, charging effects have not come into the picture. When the bias exceeds 3.0 V and μ_2 begins to get across the LUMO, the electrons start to fill the LUMO, with the energy levels above the LUMO floating up due to the charging effect. Since the energy levels below the HOMO are always occupied by electrons, so the shift effect of energy levels is not apparent. The adjustment of energy levels also tries to keep the molecule system neutral.

Figure 4(a) illustrates the *I-V* curve of PDT with the perpendicular distance of the S atom in the hollow position to Au (111) plane $d=2.0$ Å as a function of bias from -5.0 V to $+5.0$ V, using the self-consistent method, in order to compare it with the experimental results. In the low bias region from -0.5 V to $+0.5$ V, the molecule is in the linear response region due to the HOMO-LUMO gap with small DOS and small T(E,V), and the current rises slowly. The transport behavior is confirmed by Fig. 2(a). Outside the linear response region, the increasing current becomes visible in Fig. 4(a). For the bias larger than 3.0 V, the current has a steep rise due to the contributions from both HOMO and LUMO. For the bias is close to 5.0 V, the rise of current becomes slow due to the lack of the states above -3.0 eV. The *I-V* curve is symmetric for the positive and negative bias since the PDT molecule is symmetric for the left and right electrodes.

This transport picture is well described with full details by the differential conductance (dI/dV), which is defined as the derivative of the current with respect to the external bias and accurately reflects the relationship between the current and the bias. In the linear response region, there is a conductance gap within 1.0 V, in consonance with the very small current. Outside this region, the differential conductance goes up continuously in agreement with the rapid rise of the current. With the bias approaching to 5.0 V, there is a drop in the differential conductance corresponding to the diminution of

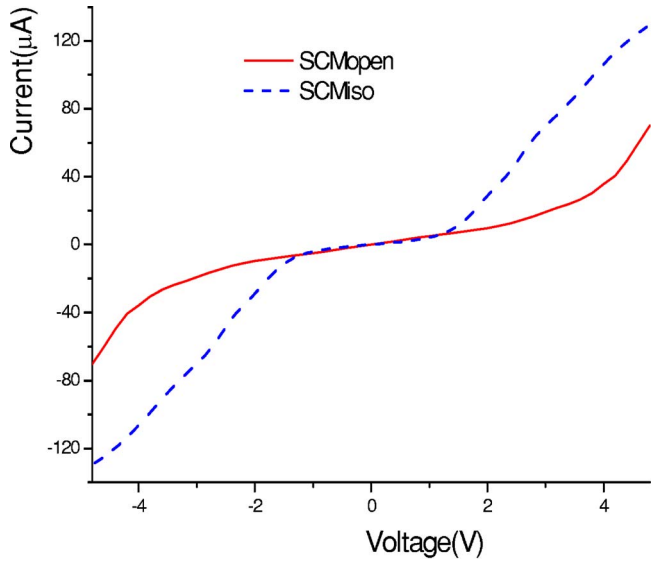

FIG. 5. (Color online) *I-V* of PDT dressed by two Au contacts with SCMiso (dashed) and SCMopen (solid).

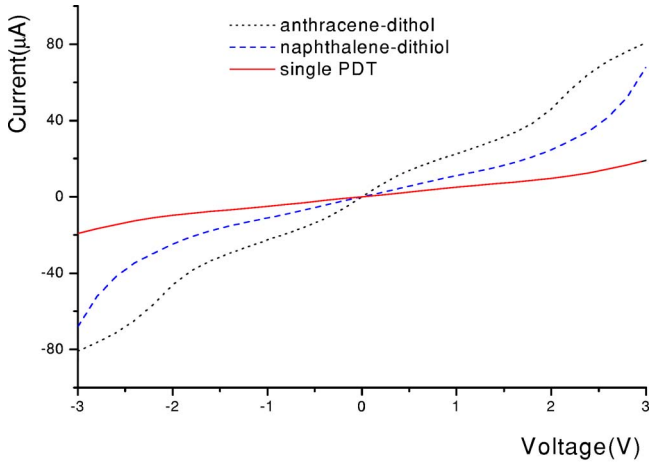

FIG. 6. (Color online) *I-V* curves of three molecule structures, anthracene-dithiol (dotted), naphthalene-dithiol (dashed), single PDT (solid). The distance between the sulfur atom and the Au (111) plane is 2.0 Å.

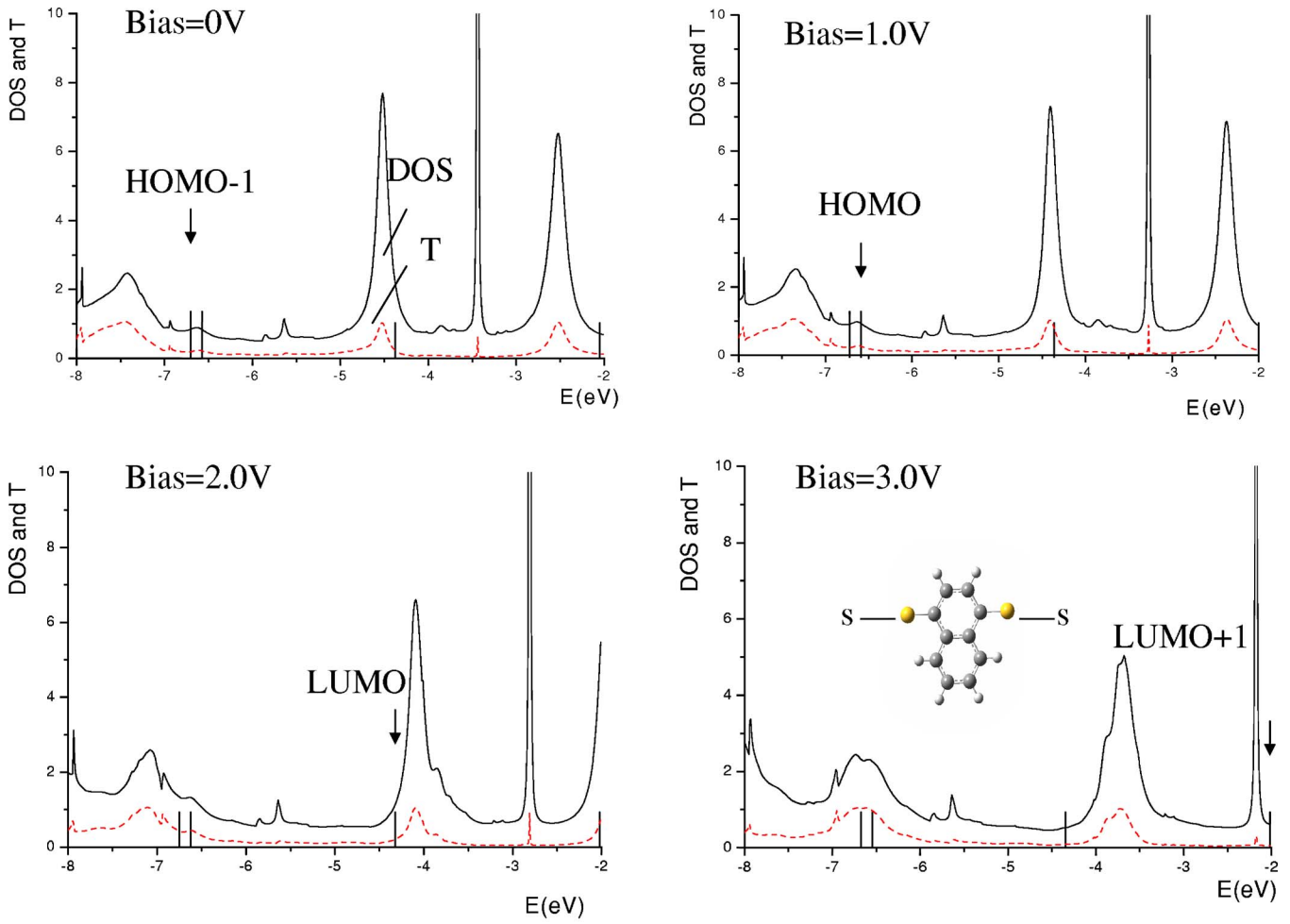

FIG. 7. (Color online) DOS and T of naphthalene-dithiol corresponding to the different biases. The distance between the sulfur atom and the Au (111) plane is 2.0 Å.

slope of the current curve. The differential conductance curve is supported by the experiment.[1] The molecule resistance makes the potential decline evenly distributed almost in the whole PDT, not just concentrated around the atoms.

Figure 5 compares the current curves obtained by the self-consistent method for the lead-molecule-lead open system under bias (SCMopen) with that for the isolated molecule in equilibrium (SCMiso), which was used for the benzene derivatives.[23] The SCMiso adopts the bulk Au DOS to construct SGF with only diagonal elements[27] and the self-consistent cycle of the isolated molecule inside Gaussian, without considering the charge transfer effect. Despite the SCMiso current (dotted line) presents the conductance gap, the invariant current slope does not lead to the experimental differential conductance, and the value of the current is almost twice as large as that of the SCMopen (solid line). With SCMiso, the transferred electron number $|\delta n| > 3.0$ shows it is a crude approximation. Compared with the SCMiso, the SCMopen illustrates the full theoretical consideration and the advantages of small current and experiment favorable differential conductance.

Though the distance between the sulfur atom and Au (111) surface plane 2.0 Å is usually acceptable, the experimentally available distance is still neither clear nor fixed. According to our calculation, the current behavior is not sensitive to small variation in the distance, for example, from 1.9 Å to 2.2 Å. The calculated results for the distance $d = 2.1$ Å are shown in Fig. 2(b) and Fig. 4(b), comparing with the result at $d = 2.0$ Å in Fig. 2(a) and Fig. 4(a). In Fig. 2(b), the broadened HOMO is closer to E_f than the broadened LUMO with the change in distance. With $d = 2.1$ Å, the transferred charges $|\delta n|$ from the molecule to the metal are also less than 0.2. In Fig. 4(b), the current value descends in comparison with Fig. 4(a), due to the decreased coupling between the molecule and the lead. But the behavior of the curve agrees with that in Fig. 4(a) qualitatively. The differential conductance, which describes the details of current, is not the same as the one in Fig. 4(a).

With the variation in the distance between the S atom and Au contact surface from 2.0 Å to 2.1 Å, the initial rise of the current all occurs at 3.0 V, but the charge carrier responsible changes from hole to electron. At the higher bias, both electron and hole contribute to the current. Our results can be compared with that of experiment qualitatively in the shape. The difference between theory and experiment is only the order. The reasonable explanation may be that we adopt chemical bond to describe the interaction between S atom and Au contact surface. In experiments the sulfur atom is

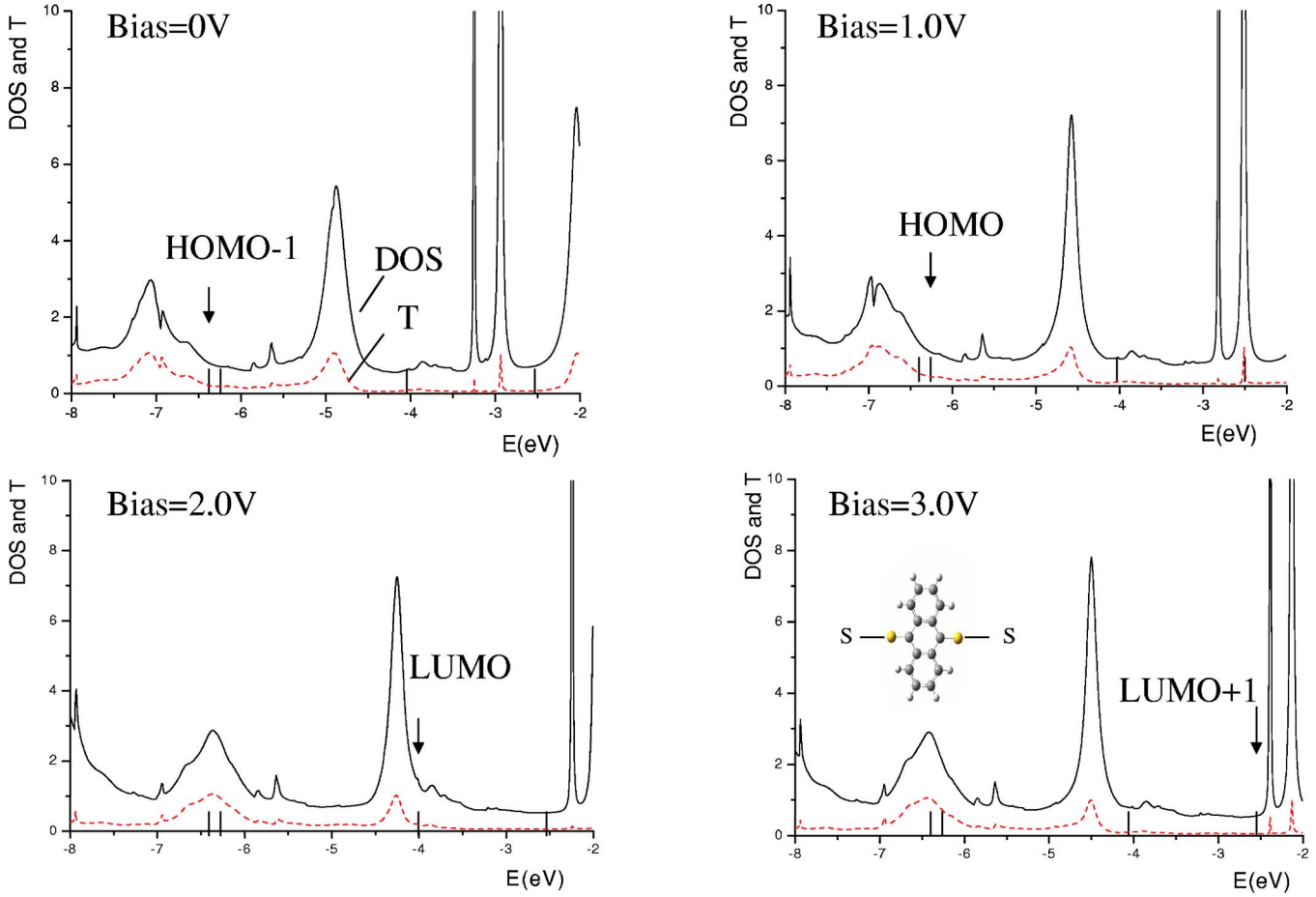

FIG. 8. (Color online) The same as Fig. 7 for anthracene-dithiol.

absorbed on surface of the gold lead by so-called self-assembly, which may have weaker coupling than the real chemical bond, that we adopted in our calculation. This may be the main reason that the measured current is smaller than the calculated results. In our calculation the S—Au coupling is fully involved in the supermolecule, therefore we treat the organical molecule as the device to save the computer time (basis LANL2DZ has 22 orbitals for each gold atom).

People realize that a single molecule is the smallest conceivable entity that could be individually designed and manipulated in the electronic devices as an active unit. As a single molecule device, PDT has virtues of small volume and good stability. But in the range of small bias, its response to external field is not sensitive enough. Therefore, we want to search for a molecule with better qualities. Many people applied benzene derivatives with the donor or/and acceptor to achieve the goal.[22,23] Another way is to search for the molecules with different configurations. As an example, the benzenes in parallel connection may present an improved device. Figure 6 presents the *I-V* characteristics, respectively, for the single PDT (solid line), naphthalene-dithiol (dashed line), and anthracene-dithiol (dotted line) from −3.0 V to +3.0 V with the distance parameter 2.0 Å by the SCM program (the configuration of the two molecules are optimized in LANL2DZ basis set). The dashed line illustrates the typical potential barrier behavior, while the dotted line shows a complicated behavior with higher current value. According to the classical view, the naphthalene-dithiol (the anthracene-dithiol) can be roughly regarded as the two (three) same resistances in parallel connection. So, the current of the naphthalene-dithiol (the anthracene-dithiol) should be about twice (three) times as much as that of the single PDT. However, the numerical calculation shows that the current value for naphthalene-dithiol or anthracene-dithiol is much larger than the classical value. It is a unique quantum (nonohmic) effect in molecule devices. The results are supported by the recent experiment results,[34] and can be explained by DOS curves and transmission function curves. In Fig. 7, the vertical lines denote the discrete energy levels of the isolated naphthalene-dithiol. HOMO−1 is −6.63 eV, HOMO is −6.61 eV, LUMO is −4.43 eV, and LUMO+1 is −2.11 eV. When the molecule is coupled to contacts, the four peaks, shifted and broadened, in the figure are HOMO, LUMO, LUMO+1, and LUMO+2 from the left to the right. The peak of DOS is continuously shifted to the high energy with bias increased, because the Fermi level is close to the LUMO in equilibrium, electrons fill the LUMO and the charging energy causes the energy levels to float up with the bias rising. The relative positions between HOMO, LUMO, and E_f makes the molecular device have the potential-barrier-like transport behavior, the linear *I-V* behavior appears after the conductance gap, for both the positive and negative biases.

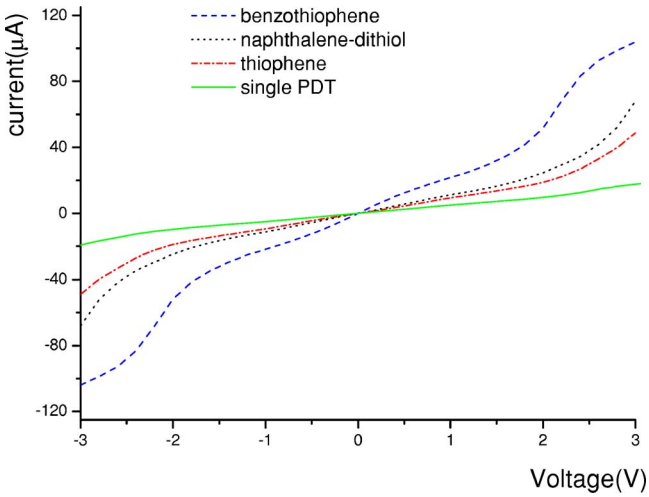

FIG. 9. (Color online) *I-V* curves of four molecule structures, benzothiophene (dashed line), naphthalene-dithiol (dotted line), thiophene (dashed-dotted line), and single PDT (solid line). The distance between the sulfur atom and the Au (111) plane is 2.0 Å.

In Fig. 8, four molecular levels of the isolated anthracene-dithiol are labelled in the different figures to avoid crowd, −6.46 eV, −6.40 eV, −4.06 eV, and −2.52 eV from HOMO −1 to LUMO+1. When anthracene-dithiol is connected to two leads, HOMO is shifted to −7.20 eV, LUMO to −4.9 eV and LUMO+1 to −3.25 eV with E_f close to the LUMO. At equilibrium the Fermi level is near the LUMO, with bias increasing from zero μ_2 grows up and fills the LUMO, the charge interactions drive the molecular levels and DOS peaks of anthracene up until μ_1 reaches across the HOMO (bias V=2.4 V) and wants to empty the HOMO, where the charge losing effect is dominant over the charge gained one and the molecular levels start to go down, especially for the LUMO.[18]

For molecular transport, not only benzene ring but also thiophene ring are the devices we focus on. A transistor fully composed of organic material was made by polythiophene in 1994.[35] In the following, we use thiophene and benzothiophene as an example to show some other complicated transport behaviors in the molecular devices. Thiophene and benzothiophene are all closed shell systems, whose valence electron number are 18, 26 respectively. Thiophene has a pentagon structure, whose bonds have different length. The S—C bonds are long bonds, 1.672 Å. The length of the other C—C bonds are 1.377 Å, 1.377 Å, 1.432 Å. When thiophene is combined with benzene in parallel, the molecule of the quinoidic structure has strong current. The bond length of benzene changes from 1.395 Å to 1.405 Å, while the length of the S—C bond is 1.830 Å, and the length of the C—C bonds are 1.467 Å, 1.405 Å, 1.467 Å in the thiophene. The SCMopen results show that the transport capacity of thiophene, the single pentagon structure, is better than PDT, the single hexagon structure. Accordingly, the current value of benzothiophene is larger than that of naphthalene-dithiol. Figure 9 describes the *I-V* curves of PDT, thiophene, naphthalene-dithiol, and benzothiophene, respectively. At the same bias, the current value of thiophene (benzothiophene) is almost twice as much as that of PDT (naphthalene-dithiol). The DOS and transmission function of thiophene and benzothiophene in Fig. 10 explain the transport results. The shifted and broadened molecular energy levels satisfy the equation $[F_M+\Sigma_1^R(E_f)+\Sigma_2^R(E_f)]\psi=ES_M\psi$. The real part of the energy level describes the shift of the energy level, while its imaginary part describes broadening. The arrowheads in Fig. 10 denote the four levels from HOMO−1 to LUMO+1 of the isolated thiophene and benzothiophene. The calculation shows that in the lead-molecule-lead system, the HOMO position of thiophene is −7.24 eV, LUMO is −3.73 eV and LUMO+1 is −2.35 eV, while the HOMO position of the benzothiophene is −7.07 eV, its LUMO is

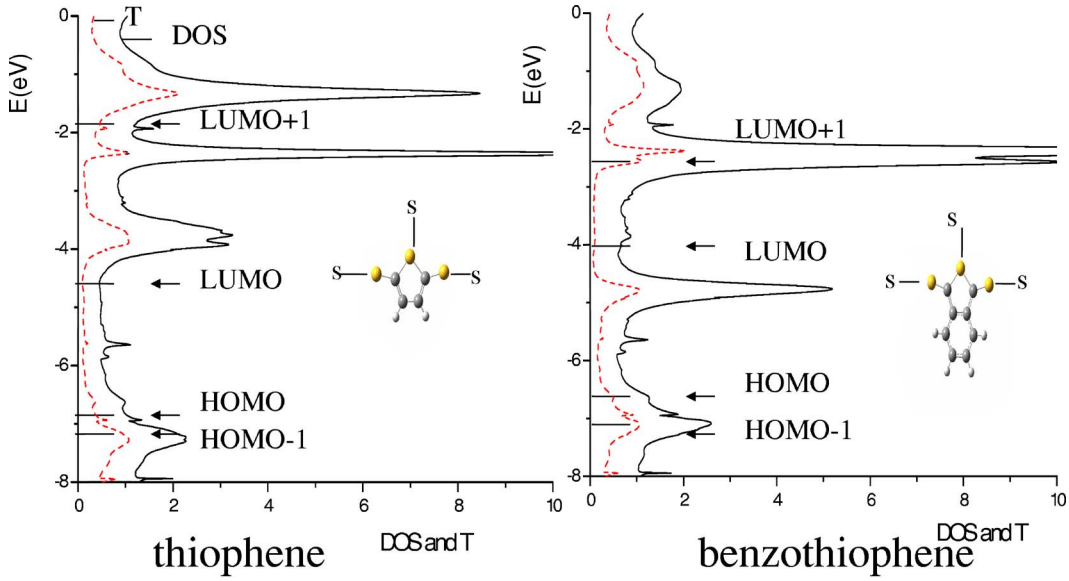

FIG. 10. (Color online) The energy levels of thiophene and benzothiophene. The horizontal line shows the energy levels of the isolated thiophene (benzothiophene). The solid line shows the broadened DOS of thiophene (benzothiophene) and the dashed line shows the transmission coefficients of thiophene (benzothiophene). The distance between the sulfur atom and the Au (111) plane is 2.0 Å.

−4.79 eV and LUMO+1 is −2.56 eV. The small peaks inside HOMO-LUMO gap in Fig. 10 are MIGS. Compared to the single PDT, the LUMO of thiophene is not localized on its ring (the LUMO peak of PDT is much sharper than that of thiophene), it participates in transport and makes its transport capacity better than that of the single PDT. So is the benzothiophene.

In a word, our results show that the current control can be realized not only by benzene derivatives but also by structure controlled assembly molecules. At present, the task of packing a large number of functional molecular devices together is the main goal in the nanoelectronic regime. Understanding the behavior of the functional molecular group is a significant step in the design of molecular devices.

IV. SUMMARY

We use the self-consistent method based the DFT and the nonequilibrium Green's function to simulate molecule transport. We expect to solve the transport problem from the first-principles theory in order to predict the transport characteristics of some molecules and identify the experimental results from the theoretical point of view. We use GAUSSIAN03 to obtain the electronic structure and at the same time, we break the self-consistent iteration cycle inside Gaussian, by replacing the density matrix of the isolated molecule with the density matrix of the open system, and run self-consistent iteration until the density matrix converges within an acceptable accuracy. By using the self-consistent method, we study the transport characteristics of PDT, the results are supported by the experiment. The study also shows that these results are not sensitive to a very small variation in the distance between the S atom and Au (111) surface plane, in spite of the different transport essence. We continue to investigate the influence on the transport due to the change in molecule structure. The numerical calculations identify that the benzene-rings in parallel connection (naphthalene-dithiol and anthracene-dithiol) show a unique quantum (nonohmic) effect. The SCM can also be used in other areas, for example, to deal with spintronic devices.[36] Therefore, it owns a bright foreground. At this stage of research work, we only focus on the coherent transport at zero temperature. Further improvements in the future work should consider the noncoherent transport at nonzero temperatures essentially in longer molecules such as DNA chains.

ACKNOWLEDGMENTS

This work is supported by the National Science Foundation of China (NSFC) under Contract No. 90206031, the National Key Program of Basic Research Development of China (Grant No. G2000067107), and Special Coordination Funds of the Ministry of Education, Culture, Sports, Science and Technology of the Japanese Government. The authors would like to thank Dr. A. Ghosh, Professor H. Guo, and Professor H.P. Cheng for helpful discussions. The authors also would like to express their sincere thanks to the support from the staff at the Center for Computational Materials Science of IMR Tohoku University for the use of the SR8000 G/64 supercomputer facilities.

*Corresponding author. Electronic address: haochen@fudan.edu.cn

[1] M. A. Reed, C. Zhou, C. J. Muller, T. P. Burgin, and J. M. Tour, Science **278**, 252 (1997).
[2] D. I. Gittins, D. Bethell, D. J. Schriffrin, and R. J. Nichols, Nature (London) **408**, 67 (2000).
[3] X. D. Cui, A. Primak, X. Zarate, J. Tomfohr, O. F. Sankey, A. L. Moore, T. A. Moore, D. Gust, G. Harris, and S. M. Lindsay, Science **294**, 571 (2001).
[4] N. B. Zhitenev, H. Meng, and Z. Bao, Phys. Rev. Lett. **88**, 226801 (2002).
[5] J. Park, A. N. Pasupathy, J. I. Goldsmith, C. Chang, Y. Yaish, J. R. Petta, M. Rinkoski, J. P. Sethna, H. D. Abruna, P. L. McEuen, and D. C. Ralph, Nature (London) **417**, 722 (2002).
[6] W. Liang, M. P. Shores, M. Bockrath, J. R. Long, and H. Park, Nature (London) **417**, 725 (2002).
[7] R. H. M. Smit, Y. Noat, C. Untiedt, N. D. Lang, M. C. van Hemert, and J. M. van Ruitenbeek, Nature (London) **419**, 906 (2002).
[8] J. Reichert, R. Ochs, D. Beckmann, H. B. Weber, M. Mayor, and H. v. Löhneysen, Phys. Rev. Lett. **88**, 176804 (2002).
[9] R. H. M. Smit, C. Untiedt, G. Rubio-Bollinger, R. C. Segers, and J. M. van Ruitenbeek, Phys. Rev. Lett. **91**, 076805 (2002).
[10] D. Dulic, S. J. van der Molen, T. Kudernac, H. T. Jonkman, J. J. D. de Jong, T. N. Bowden, J. van Esch, B. L. Feringa, and B. J. van Wees, Phys. Rev. Lett. **91**, 207402 (2003).
[11] B. Xu and N. J. Tao, Science **301**, 1221 (2003).
[12] B. Xu, X. Xiao, and N. J. Tao, J. Am. Chem. Soc. **125**, 16164 (2003).
[13] X. Xiao, B. Xu, and N. J. Tao, Nano Lett. **4**, 267 (2003).
[14] W. Tian, S. Datta, S. H. Hong, R. Reifenberger, J. I. Henderson, and C. P. Kubiak, J. Chem. Phys. **109**, 2874 (1998).
[15] M. Di Ventra, S. T. Pantelides, and N. D. Lang, Phys. Rev. Lett. **84**, 979 (2000).
[16] Y. Xue and M. A. Ratner, Phys. Rev. B **68**, 115406 (2003).
[17] P. S. Damle, A. W. Ghosh, and S. Datta, Phys. Rev. B **64**, 201403(R) (2001).
[18] P. S. Damle, A. W. Ghosh, and S. Datta, Chem. Phys. **281**, 171 (2002).
[19] J. Taylor, H. Guo, and J. Wang, Phys. Rev. B **63**, 245407 (2001).
[20] M. Brandbyge, J. L. Mozos, P. Ordejón, J. Taylor, and K. Stokbro, Phys. Rev. B **65**, 165401 (2002).
[21] K. Stokbro, J. Taylor, M. Brandbyge, J. L. Mozos, and P. Ordejón, Comput. Mater. Sci. **27**, 151 (2003).
[22] J. Chen, M. A. Reed, A. M. Rawlett, and J. M. Tour, Science **286**, 1550 (1999).
[23] H. Chen, J. Q. Lu, J. Wu, R. Note, H. Mizuseki, and Y. Kawazoe, Phys. Rev. B **67**, 113408 (2003).
[24] T. Tada, M. Kondo, and K. Yoshizawa, J. Chem. Phys. **121**, 8050 (2004).
[25] M. Kondo, T. Tada, and K. Yoshizawa, J. Chem. Phys., **108**, 9143

(2004).
[26] C. Zhang, M. H. Du, H. P. Cheng, X. G. Zhang, A. E. Roitberg, and J. L. Krause, Phys. Rev. Lett. **92**, 158301 (2004).
[27] P. A. Derosa and J. M. Seminario, J. Phys. Chem. B **105**, 471 (2001).
[28] F. Evers, F. Weigend, and M. Koentopp, Phys. Rev. B **69**, 235411 (2004).
[29] P. Delaney and J. C. Greer, Phys. Rev. Lett. **93**, 036805 (2004).
[30] Z. Yuan, C. R. Su, S. Z. Zhang, and J. M. Li, Chin. Phys. Lett., **21**, 568 (2004).
[31] N. Vedova-Brook, N. Matsunaga, and K. Sohlberg, Chem. Phys., **299**, 89 (2004).
[32] M. J. Frisch *et al.*, GAUSSIAN03, Revision B. 04, Gaussian, Inc., Pittsburgh, PA, 2003.
[33] F. Zahid, M. Paulsson, and S. Datta, in *Advanced Semiconductors and Organic Nano-Techniques III*, edited by H. Morkoc (Academic, San Diego, 2003).
[34] M. H. Zareie, H. Ma, B. Reed, A. Y. Jen, and M. Sarikaya, Nano Lett., **3**, 139 (2003).
[35] F. Garnier, R. Hajlaoui, A. Yassar, and P. Srivastava, Science, **265**, 1684 (1994).
[36] R. Pati, L. Senapati, P. M. Ajayan, and S. K. Nayak, Phys. Rev. B **68**, 100407(R) (2003).